

A global analysis of cross-talk in a mammalian cellular signalling network

Madhusudan Natarajan^{1,2}, Keng-Mean Lin^{1,2}, Robert C. Hsueh^{1,2}, Paul C. Sternweis^{1,2} and Rama Ranganathan^{1,3,4}

Cellular information processing requires the coordinated activity of a large network of intracellular signalling pathways. Cross-talk between pathways provides for complex non-linear responses to combinations of stimuli, but little is known about the density of these interactions in any specific cell. Here, we have analysed a large-scale survey of pathway interactions carried out by the Alliance for Cellular Signalling (AfCS) in RAW 264.7 macrophages. Twenty-two receptor-specific ligands were studied, both alone and in all pairwise combinations, for Ca²⁺ mobilization, cAMP synthesis, phosphorylation of many signalling proteins and for cytokine production. A large number of non-additive interactions are evident that are consistent with known mechanisms of cross-talk between pathways, but many novel interactions are also revealed. A global analysis of cross-talk suggests that many external stimuli converge on a relatively small number of interaction mechanisms to provide for context-dependent signalling.

To define 'complexity' in terms of cellular signalling consider all possible combinations of input stimuli that might initiate signalling events in a cell as a set of unique 'messages' that can be sent by the external environment. Even if we simplify the analysis by treating stimuli as binary inputs, the number of such messages grows dramatically with the number of stimuli — for even 20 inputs, over a million possible unique combinations are possible. How does a cell process this enormous number of potential messages in making output responses? At the limit of minimal complexity, signalling events initiated by ligands could be entirely independent of one another, with no cross-talk or mutual influence. In this case, the response to any combination of stimuli requires knowledge of only the single ligand responses as any unsaturated response must be simply a linear, weighted summation of these responses. This mechanistic independence of transduction events does not prevent the cell from having many output states to combinations of stimuli — it only means that all the output states are predictable from combinations of single ligand responses. At the limit of maximal complexity, however, the responses of ligands would be fully context-dependent; that is, the response to any given ligand depends on the specific background of others. In this case, the total cellular response to any combination of stimuli is fundamentally unpredictable from responses to other combinations of ligands. Each ligand combination produces an irreducible unique output state and knowledge of single ligand response is insufficient to describe any of these states.

This operational definition of complexity — the unpredictability of responses to arbitrary combinations of stimuli given knowledge of responses to their simpler combinations — is intimately linked to the

wiring complexity of the underlying signalling system. The more unpredictable the response to combinations of stimuli, the more interconnected and structurally complex the transduction network must be. To provide an experimental assessment of functional interactions between stimuli in one cell type, the Alliance for Cellular Signalling (AfCS, <http://www.signaling-gateway.org/>)¹ carried out systematic measurements of output responses of RAW 264.7 macrophages to the application of 22 receptor-specific ligands and all 231 pairwise combinations of these ligands. The ligands were identified through examination of the literature, receptor expression studies and preliminary dose-response experiments (see Supplementary Information, Fig. S1). Selected agonists provide for stimulation of a diverse set of signalling pathways (Toll-like receptors (TLRs), G protein-coupled receptors (GPCRs), cytokine receptors and tyrosine kinase receptors; see Supplementary Information, Table S1), many of which are co-activated during physiological signalling events (see Supplementary Information, Table S2). Output measurements fell into two categories: (1) final outputs, comprised of measurements of secretion of 18 cytokines; and (2) intermediate outputs, comprised of the kinetics of intracellular calcium mobilization and cAMP synthesis and the phosphorylation of 21 signalling proteins. Analysis of these data describe a basic architecture of the signalling network in which only a few input stimuli are able to independently control cellular outputs and the majority of inputs primarily act as modulators of signalling. The data suggest that the regulatory cross-talk between signalling cascades may be comprised of a limited number of interaction mechanisms and thus provide the basis for a systematic dissection of these mechanisms.

¹Department of Pharmacology, University of Texas Southwestern Medical Center, Dallas, TX 75390–9050, USA. ²The Alliance for Cellular Signalling, University of Texas Southwestern Medical Center, Dallas TX 75390, USA. ³Howard Hughes Medical Institute, University of Texas Southwestern Medical Center, Dallas, TX 75390–9050, USA. ⁴Correspondence should be addressed to R.R. (e-mail: rama.ranganathan@utsouthwestern.edu)

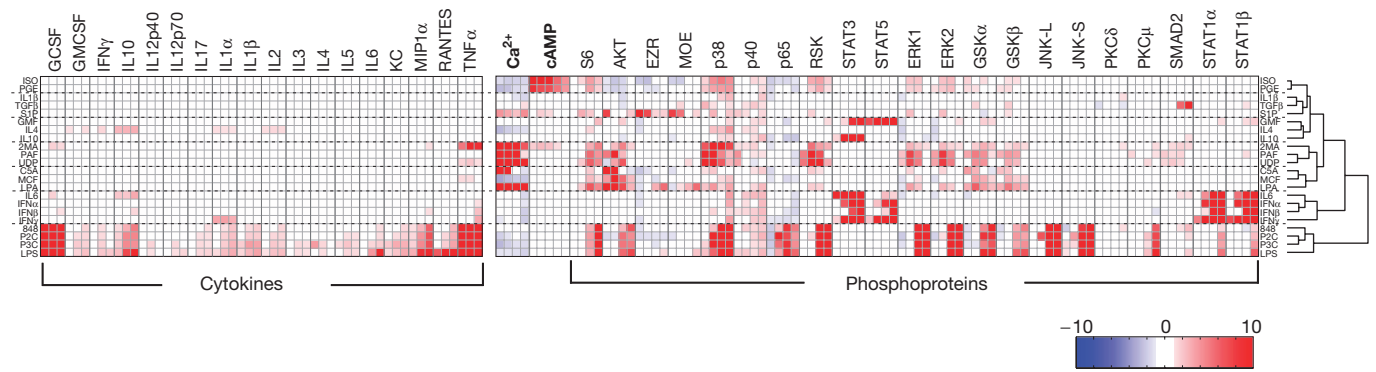


Figure 1 The single ligand screen in RAW 264.7 cells. The matrix shows the experimental responses (columns) of RAW cells to stimulation with the 22 ligands (rows) that comprise the scope of the AfCS study. Responses are in Z-scores (see text) that represent the number of standard deviations that each experimental result is removed from unstimulated controls. Each block of columns represents a time series of observation (Ca²⁺ – rising

phase and peak, initial falling phase, slow decay to steady state, plateau; cAMP – 0.33, 0.66, 1.5, 5 and 20 min; phosphorylation – 1, 3, 10 and 30 min; cytokine production – 2, 3 and 4 h). The matrix is hierarchically clustered by ligand, with functional groups divided by dashed lines. The colour scale ranges from -10σ (blue) to $+10\sigma$ (red), with all insignificant values within $\pm 1\sigma$ in white.

RESULTS

The single ligand screen

A clustered matrix representation of the single ligand screen — the profiling of output responses to all 22 ligands applied individually — is shown in Fig. 1. Each pixel of the matrix shows the mean signal for one experimentally measured variable (a column) on stimulation with one ligand (a row). The measured variables came from several experimental assays that differed in units of measurement, signal-to-noise ratio and intrinsic day-to-day variability — for example, measurements of intracellular Ca²⁺ (in nM) were typically rapid (seconds), showed good dynamic range and were sampled every 3 s for 10 min. In contrast, measurements of phosphoprotein responses (fold change over basal) over a time-scale of many minutes showed relatively weaker dynamic range, and were sampled only four times over 30 min. Thus, we transformed all raw measurements into Z-scores to provide a uniform statistical representation of the data suitable for comparison (see Methods). Hierarchical clustering reveals a robust classification of ligands into known functional groups (separated by dotted lines) on the basis of their output response profiles. Ligands for the TLRs, lipopolysaccharide (LPS), PAM2CSK4 (P2C), PAM3CSK4 (P3C) and resiquimod (848) emerge as a single cluster distinguished by their dominant action in cytokine secretion and similar patterns of protein phosphorylation. TLRs signal through the proximal adaptor protein MyD88, which results in activation of NF- κ B and MAP kinase pathways². Consistent with this, Z-scores for the TLR ligands show time-evolving phosphorylation of an NF- κ B signalling component (p65 subunit), ribosomal S6 protein and S6 kinase (RSK), proteins in the phosphatidylinositol-3-OH-kinase (PI(3)K) pathway (Akt, GSK α and GSK β) and MAP kinase signalling proteins (p38MAPK, ERK1, ERK2, JNKL, JNKS), as well as cytokine production. The interferons (IFNs: IFN α , IFN β and IFN γ) cluster with interleukin 6 (IL6) by their pattern of STAT phosphorylation³. GPCR agonists isoproterenol (ISO) and prostaglandin E2 (PGE) cluster together due to their strong cAMP responses. 2-methylthio-ATP (2MA), platelet activating factor (PAF) and uridine diphosphate (UDP) cluster together by strong Ca²⁺ and phosphoprotein responses^{4,5}. Other GPCR agonists, lysophosphatidic acid (LPA) and complement C5A, cluster with the tyrosine kinase receptor agonist macrophage colony stimulating factor (MCF). In general, the single ligand matrix shows excellent consistency with known signalling mechanisms and classifies

ligands into functional groups based on characteristic ligand signature responses — a finding that provides confidence in the analytic method for assembly of disparate experimental data into a single output response profile.

The double ligand screen

To evaluate cross-talk between pathways, the AfCS also carried out the so-called ‘double-ligand’ screen. This experiment was designed to measure output responses for all ligands applied both singly and in pairwise combinations in matched experiments (231 combinations for 21 ligands). If two ligands act independently to alter any particular output variable, then the response to their combined application is expected to be the additive effect of applying them individually. If the combined application produces a value that is different from that expected from addition of their individual applications, then the two ligands interact by that output variable and to the extent measured by the difference. Appropriately weighted for propagated errors of measurement, this ‘non-additivity’ ($\Delta\Delta Z$; see Methods) is the quantitative measure of cross-talk between a pair of transduction events. It is worth noting that this type of analysis of cross-talk can detect interactions between signalling pathways, but remains largely unbiased with regard to the underlying molecular mechanisms. Indeed, cross-talk may be achieved through multiple mechanisms ranging from direct communication between intracellular pathways to more indirect feedback processes such as autocrine signalling. Regardless of mechanism, all of these processes contribute to the complexity of unique signalling states in cells and therefore fall into the sphere of interest of the double-ligand screen experiment.

Examples of non-additivity between ligand responses in RAW cells are shown (Fig. 2). Each panel indicates the experimentally observed effects on one variable of a pair of ligands applied either individually (in black) or together (in red). The curve in blue represents the signal expected for the combined addition of the two ligands if they act independently; thus, the difference between the red and blue curves indicates the degree of non-additivity. C5A and UDP both mobilize Ca²⁺, but the combined effect of the two is greater than that expected for their independent action at the peak of the calcium transient (Fig. 2a). Thus, C5A and UDP show synergy in signalling — one manifestation of cross-talk. ISO elevates intracellular cAMP markedly, whereas sphingosine-1-phosphate (S1P) does not (Fig. 2b). However, ISO and S1P

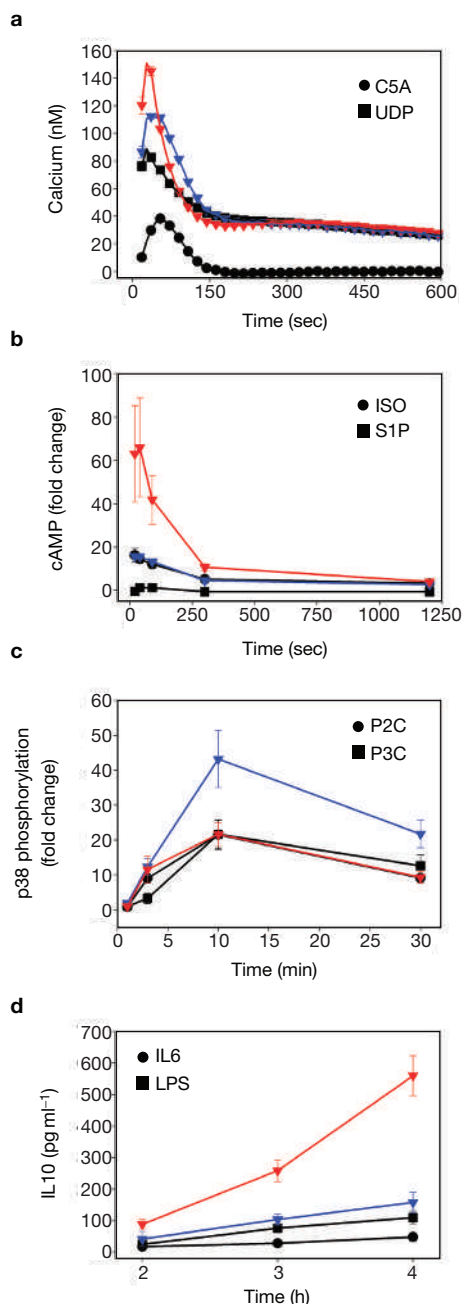


Figure 2 Non-additivity between pairs of ligands applied to RAW 264.7 cells in all four experimental assays. Each panel shows the effects of two ligands applied individually (black; see legend for ligands) or applied together (red). The calculated additive response for independent simultaneous action of the two ligands is shown in blue. The difference between the observed effect of combined addition of two ligands (the red curve) and the expected effect in the case that the ligands act independently (blue curve) is the degree to which the two ligands interact. Note that the interaction could be either positive (a, b, d) or negative (c). Error bars in all plots represent standard error of mean ($n = 3-7$ depending on assay). In panel a, symbols are shown every 10 data points.

synergize to produce a much greater than expected effect in the early phase of cAMP production. P2C and P3C both stimulate p38 MAPK phosphorylation, but the effect of the simultaneous addition of the two produces the same level of p38 phosphorylation as each ligand applied alone (Fig. 2c), suggesting saturation of a common upstream signalling

component, another manifestation of cross-talk. Finally, IL6 and LPS alone both induce IL10 production, but show synergistic secretion of IL10 when combined (Fig. 2d).

Because of its size, the complete double ligand screen for all 231 ligand pairs in the RAW 264.7 cell is provided as supplementary information (see Supplementary Information, Fig. 2). Fig. 3 shows a subset of these data that allow validation of the analytic methods against known mechanisms of cross-talk and that demonstrate novel predictions. The data are shown as a matrix of $\Delta\Delta Z$ interaction scores for many pairs of ligands (rows) for all experimental variables (columns). Thus, each pixel indicates the degree of non-additivity for one ligand pair in one experimental measurement. For clarity, we have numbered pixels in Fig. 3 by order of presentation below. Note that most numbers highlight multiple pixels.

Interactions between all pairs of TLR ligands show systematic less-than-additive effects on many cytokines and on components of MAPK, PI(3)K and NF- κ B pathways (Fig. 3a), consistent with known mechanisms of stimulation and saturation of known pathways^{6,7}. As expected, TLR ligands also cooperatively interact with IFN γ and IFN β ⁸⁻¹⁰, giving greater-than-additive IL6 and RANTES production (1). The LPS-IFN β synergism is more muted (1), which may be accounted for by auto-crine effects of LPS-induced IFN β production that blunt the response to exogenously added interferon¹¹. Interestingly, IFN β -TLR but not IFN γ -TLR combinations show synergistic IL10 production (2) consistent with the notion that Type I IFNs selectively promote the anti-inflammatory actions of macrophages¹². Moreover, consistent with its close clustering with the Type I IFNs in the single ligand screen (Fig. 1) and its anti-inflammatory action¹³, IL6 also interacts with TLRs to stimulate IL10 production (3) and to suppress TNF α release (3). All IFN-TLR and TLR-IL6 combinations show reduced STAT1 and STAT3 phosphorylation at 30 min (4, 5), a result consistent with findings that TLR signalling leads to delayed inhibition of select cytokine signalling through production of suppressors of cytokine signalling (SOCS) proteins^{14,15}.

ISO and PGE decreased the production of TLR-induced cytokines MIP1 α and TNF α (6), corroborating a known ISO-mediated decrease of LPS-induced TNF α production¹⁶. Interestingly, these ligand combinations also show increased GCSF and IL10 production (7), supporting the general notion that GPCR signalling through G α s counteracts the TLR-mediated inflammatory response¹⁷⁻¹⁹. A specific interaction was observed for PGE and the TLR ligand P3C in synergistic IL6 production (8); this interaction has been previously described and it is argued that the suppression of TNF α production is in part mediated by increased IL6 production²⁰. In summary, analysis of the $\Delta\Delta Z$ matrix demonstrates strong consistency with available knowledge of interactions between signalling pathways.

New interaction mechanisms derived from the $\Delta\Delta Z$ interaction matrix

The $\Delta\Delta Z$ interaction matrix also demonstrates novel interactions between signalling pathways. Consider the interactions between ligands inducing cAMP production (ISO, PGE) and Ca²⁺-mobilizing ligands (2MA, C5A, LPA, PAF and UDP; Fig. 3). Nearly all combinations of these ligand groups cause synergistic increases in cAMP (9) coupled with synergistic inhibition of Ca²⁺ mobilization (10). These data strongly suggest a general mutual feedback interaction between these second messenger systems in RAW 264.7 cells in which receptor-stimulated Ca²⁺

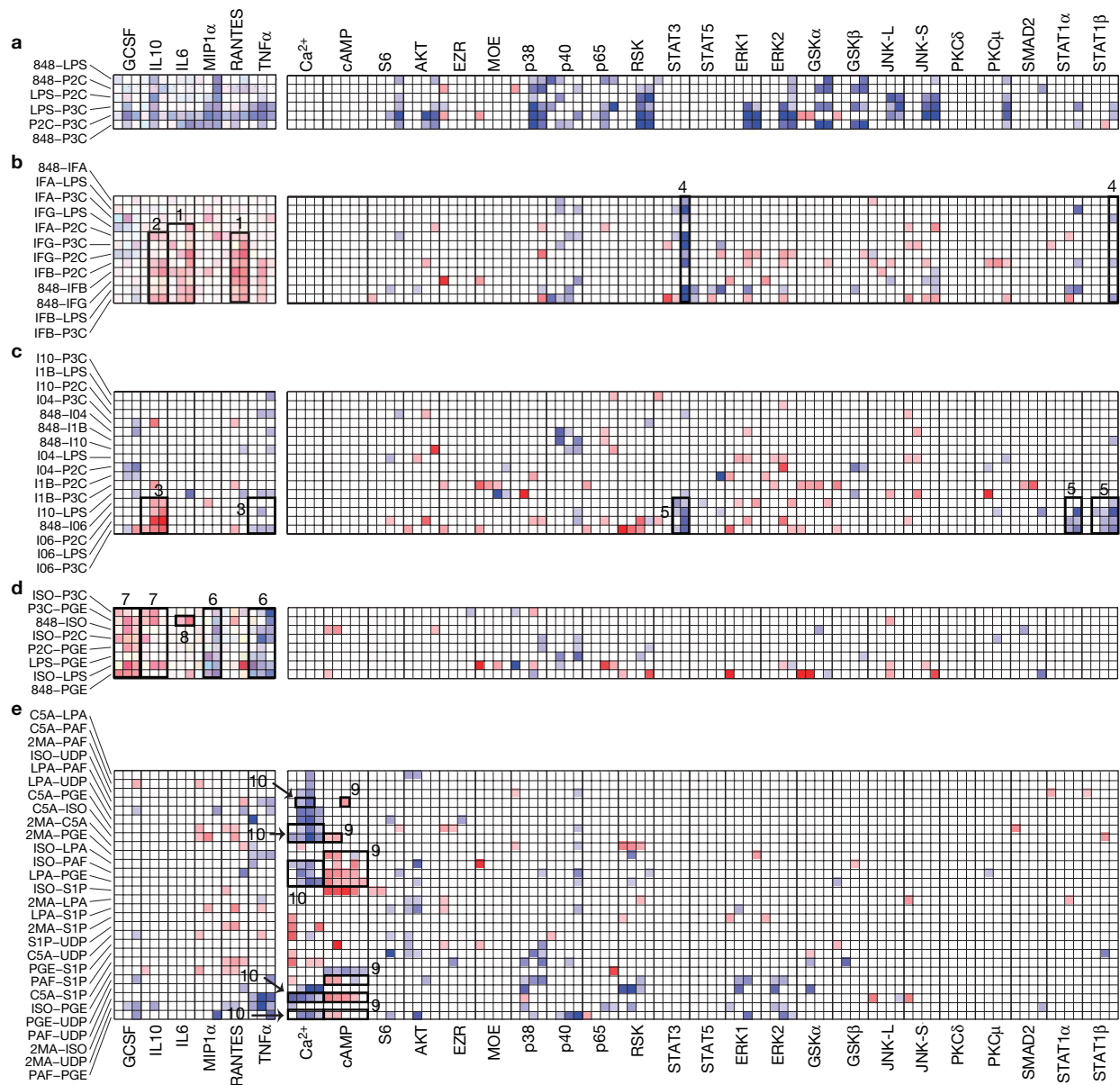


Figure 3 A subset of the double ligand screen in RAW 264.7 cells. The matrix shows the interactions between many ligand pairs (rows) for all experimental measurements (columns). The interaction is measured in $\Delta\Delta Z$ scores, which quantitatively report the non-additivity of responses to a pair of ligands (see text) in dimensionless units. The matrix is divided by receptor classes: **a**, TLR-TLR combinations; **b**, interferon-TLR

combinations; **c**, cytokine-TLR combinations; **d**, GPCR-TLR combinations; and **e**, GPCR-GPCR combinations. Specific interactions discussed in the text are highlighted in black boxes and numbered according to the order of discussion in the text. Note that most numbers highlight multiple pixels. The colour scale for $\Delta\Delta Z$ ranges from -5σ (blue) to $+5\sigma$ (red), with all insignificant values within $\pm 1\sigma$ in white.

elevation potentiates cAMP production, and cAMP in turn antagonizes Ca^{2+} mobilization. No single ligand or single perturbation analysis could have revealed this process as it is fundamentally defined by the cooperative interaction between two active signalling pathways. Thus it is only revealed in the double ligand experiment. We use the term ‘interaction agent’ to describe a signalling circuit that is uniquely involved in the coupling of distinct signalling pathways. By providing context dependence of signalling events and increasing the number of irreducible signalling states, interaction agents increase the total processing complexity of the signalling network in cells.

To better understand the Ca^{2+} -cAMP interaction mechanism, we examined how the non-additivity between Ca^{2+} and cAMP signalling

is affected by perturbation of intracellular calcium and cAMP levels (Fig. 4). ISO-mediated cAMP increase is potentiated by the presence of UDP, a Ca^{2+} -stimulating agonist (Fig. 4a; compare dark grey and black bars). This synergy persists for approximately 90 s, consistent with the time course of the UDP-dependent calcium response in RAW 264.7 cells. Pretreatment of cells with 1 μM thapsigargin, an agent that depletes intracellular stores of Ca^{2+} by inhibiting re-uptake through Ca^{2+} -ATPases, partially inhibited the synergy (Fig. 4a, yellow bars), supporting a causal link between Ca^{2+} mobilization and potentiation of cAMP production by ISO. Pretreatment of cells with 2 mM extracellular EGTA, a calcium chelator, did not inhibit the synergy at early times (20 s), but inhibited at later times (40 and 90 s), consistent with

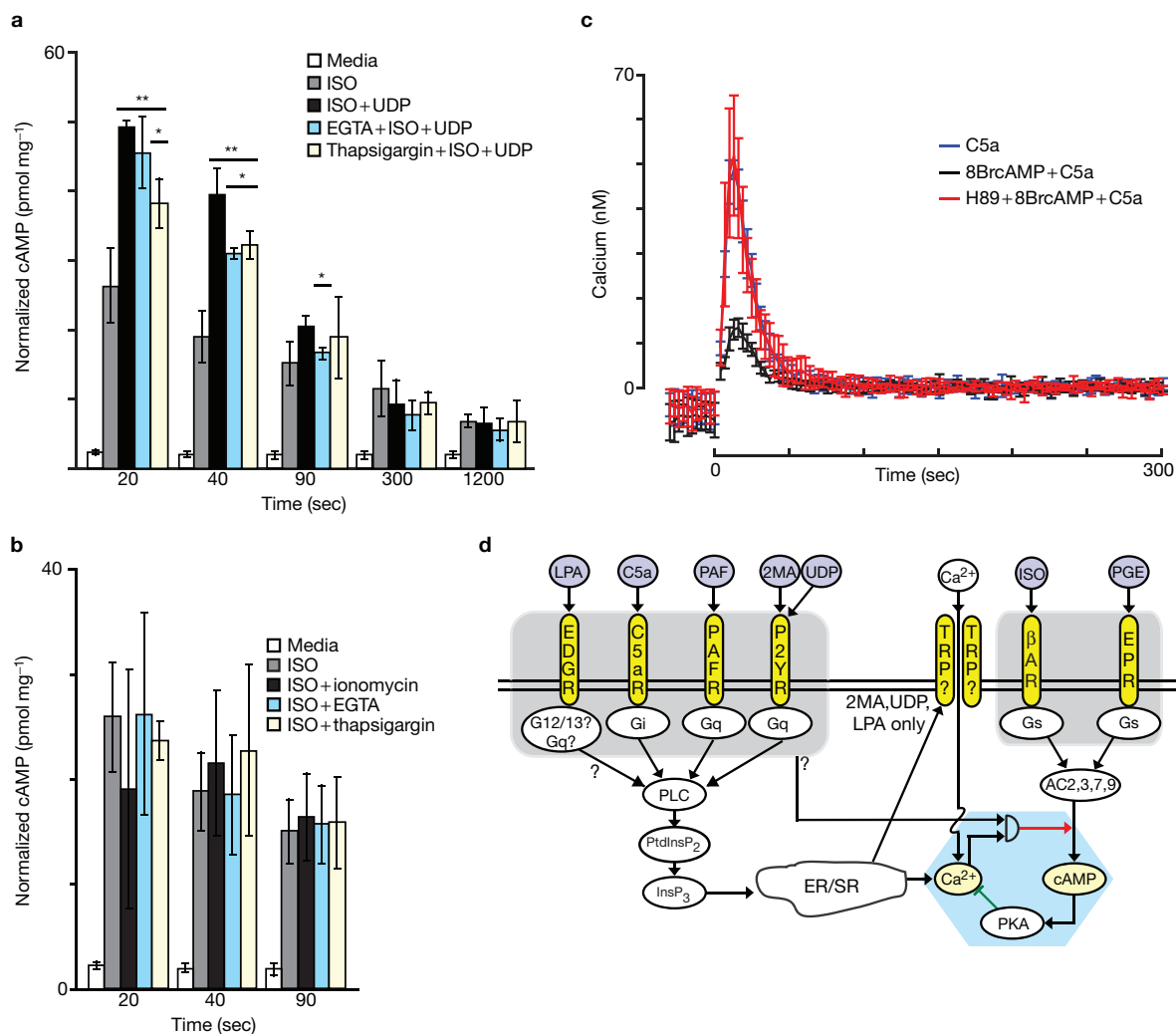


Figure 4 Testing the predicted interaction agent between calcium and cAMP. **(a)** Histograms represent normalized cAMP responses (mean \pm s. d., $n = 3$) to stimulations with ISO (dark grey), ISO + UDP (black), and to ISO + UDP after pretreatment with EGTA (light blue) or thapsigargin (light yellow). Responses that were statistically different ($P < 0.05$) from ISO and ISO + UDP are indicated (double and single asterisk, respectively). All responses were statistically significant from media alone (white). **(b)** Normalized cAMP responses (mean \pm s. d., $n = 3$) to stimulation with ISO alone (dark grey) or following pretreatment with either ionomycin (black), EGTA (light blue) or thapsigargin (light yellow) are shown. Responses on pretreatment were not statistically different from ISO alone. All treatments were significantly elevated over responses to media alone (white). **(c)** The time course of intracellular

calcium levels in response to C5a (blue, mean \pm s. d., $n = 6$), was significantly inhibited by 8BrcAMP (black). Pretreatment with H89 (red) blocked the inhibitory influence of 8BrcAMP. **(d)** A schematic representation of the interaction agent mediating cross-talk between Ca²⁺ and cAMP. GPCR ligands (blue ovals) act on cognate receptors (dark yellow ovals; grouped by Ca²⁺ and cAMP stimulators) and activate appropriate G α -subunits and subsequent signalling cascades (all signalling shown as black arrows). A receptor-dependent Ca²⁺ increase (symbolized as a logical AND gate) synergizes (red arrow) with the G α -stimulated production of cAMP. Feedback from cAMP inhibits levels of intracellular calcium by a PKA-dependent mechanism (green line). An interaction agent summarizing and defining the conditional cross-talk between Ca²⁺ and cAMP is highlighted by a blue hexagon.

the observation that UDP-dependent intracellular calcium mobilization comes in two phases — initial release from thapsigargin-sensitive intracellular stores followed by influx through plasma membrane calcium channels (Fig. 4a, blue bars). Pretreatment of cells with thapsigargin, EGTA or 2 μ M ionomycin (a calcium ionophore that raises intracellular calcium to an extent similar to that induced by UDP) also had no effect on ISO-mediated cAMP production (Fig. 4b; light yellow, blue and black bars, respectively). Thus, calcium mobilization alone, in the absence of receptor stimulation, is insufficient to support synergistic control of ISO signalling. Taken together, these results indicate that ISO-mediated cAMP production is specifically upregulated by receptor-mediated calcium mobilization.

The mechanisms by which increase in cAMP production leads to suppression of receptor-mediated intracellular calcium mobilization were further explored. The GPCR agonist C5a induces a large transient elevation in intracellular calcium (Fig. 4c, blue), but in cells pretreated with a cell-permeable, non-hydrolysable analogue of cAMP (8BrcAMP, 2 mM), this response was significantly attenuated (Fig. 4c, black). Interestingly, the effect of 8BrcAMP could be completely blocked by the pretreatment of cells with 12.5 μ M H89, a selective inhibitor of protein kinase A (PKA; Fig. 4c, red). These data argue that cAMP-mediated control of calcium signalling operates through a PKA-dependent process.

Taken together, these data provided an initial mechanistic model for a novel signalling circuit that represents the Ca²⁺–cAMP interaction agent

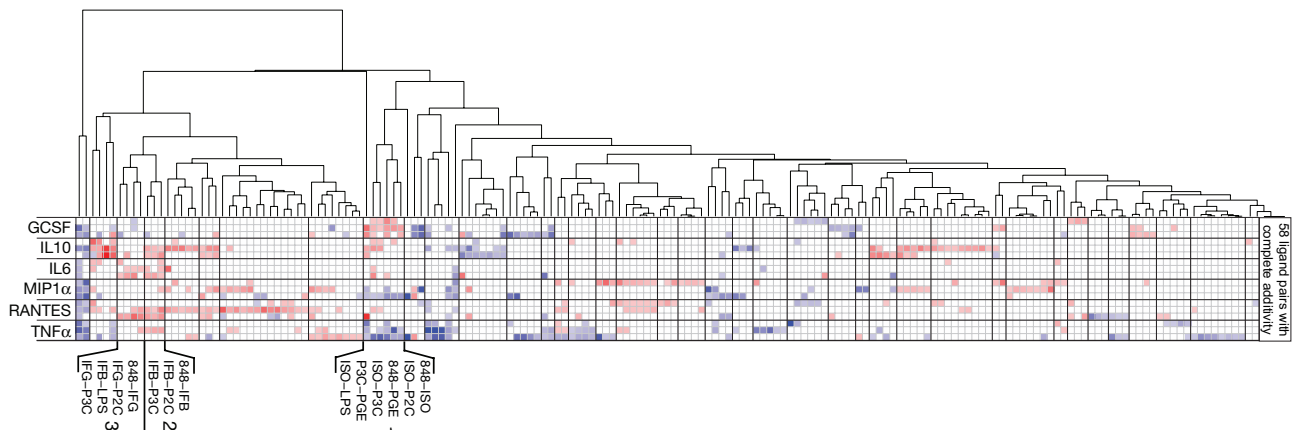


Figure 5 The complete double ligand screen in RAW 264.7 cells describing non-additivity in the secretion of cytokines in response to all 231 pairwise combinations of 22 input ligands. The matrix is hierarchically clustered, and follows the same colour scheme in Fig. 3. Ligand pairs for select clusters (labelled 1–3) are displayed (see Supplementary Information, Fig. S2 for

all labels). Analysis of clustering patterns shows that the primary effect of most ligands is exerted through modulation of cytokine production as against direct control; for example, cluster 1 shows that IFNs, which do not directly stimulate significant production of cytokines (Fig. 1), are capable of significant modulation of TLR-induced cytokine release.

(Fig. 4d, blue hexagon). Receptor-mediated elevations of intracellular calcium lead to potentiation of concurrent cAMP signalling. In turn, cAMP production operates through activation of PKA to inhibit receptor mediated Ca^{2+} mobilization. Further work will be necessary to completely expose the details of operation of this circuit, but these data serve to illustrate the core concept of the interaction agent — a network of signalling reactions that are silent during single pathway signalling events, but that become active during the simultaneous activation of multiple signalling pathways and provide the capacity for context dependence of signal processing. Analysis of the $\Delta\Delta Z$ interaction matrix is one practical experimental approach for recognizing these interaction agents and for designing new experiments to mechanistically understand them.

A global assessment of signalling cross-talk

To examine the total density of cross-talk between signalling pathways, we performed a complete assessment of non-additive interactions for all 231 ligand pairs, focused on the six cytokines that represent the significant final outputs of RAW 264.7 cells in our screen (Fig. 5). The matrix shows the non-additivity in the production of these cytokines (rows) for all ligand pairs (columns) and is clustered so that ligand pairs displaying a similar pattern of non-additivity are grouped together. The statistical significance of clusters was assessed by comparing the clustering of the actual data with that resulting from 1000 trials of randomly scrambling the $\Delta\Delta Z$ matrix (see Supplementary Information, Fig. 3 and Methods). Significant clusters are indicated by bold divisions.

The data show that all of the 22 ligands that are included in this study display at least one non-additive interaction with another ligand in modulating cytokine production (Fig. 5, columns and see Supplementary Information, Fig. S2). Similarly, every cytokine is apparently subject to both synergistically-positive and synergistically-inhibitory regulation through distinct pairwise combination of ligands (Fig. 5, rows and see Supplementary Information, Fig. S2). This is true despite the fact that many of these ligands failed to show any effect on cytokine production when applied individually (for example, ISO, PGE, and $\text{TGF}\beta$; Fig. 1). Thus we conclude that: first, interactions are many, providing a rich capacity for context dependent signalling in RAW 264.7 cells; and second, that the physiological role of most signalling pathways is not autonomous

control over main cellular outputs, but is instead context-dependent regulation of a few signalling pathways that can exert direct control.

At first glance, the finding that there are many pairwise interactions between ligands suggests the possibility that a vast number of interaction agents exists, each serving to mediate the synergistic activity of unique ligand combinations. However, the clustering of the $\Delta\Delta Z$ matrix suggests otherwise. Though many non-additive interactions are evident, ligand pairs fall into a modest number of clusters (approximately 40) based on the pattern of non-additivity (Fig. 5). These observations lead to the hypothesis that clusters represent the convergence of signalling pathways onto a small set of interaction mechanisms that combine to yield a limited number of unique cytokine regulatory programs. For example, consider cluster 1 in Fig. 5, which comprises TLR agonists paired with the GPCR ligands ISO and PGE. Activation of TLR signalling on its own leads to strong increases in production of all the cytokines included in this analysis (Fig. 1). However, according to the clustering, the coincident activity of a GPCR that mobilizes cAMP leads to a unique cytokine expression program that could not have been predicted from knowledge of the TLR or GPCR ligand responses taken independently: GCSF, IL6, RANTES and IL10 are variously potentiated, and MIP1 α and TNF α are suppressed. Note that no other cluster shows this cytokine expression program; it is a specific feature of these ligand combinations alone. These results suggest the existence of a generic interaction agent that links cAMP production to the specific modulation of TLR signalling.

To test this, we examined the effect of LPS, a TLR agonist, on production of these six cytokines with or without treatment of cells with 8BrcAMP (Fig. 6a). The data confirm that cAMP elevation is sufficient to induce the same modulation of TLR signalling to yield the same cytokine expression pattern as in the double-ligand experiment. The modulatory effects of cAMP are also demonstrated at the gene expression level (<http://www.signaling-gateway.org/data/micro/cgi-bin/micro.cgi>); application of LPS alone induces cytokine and other genes, ISO or PGE do little on their own, but the costimulation with either ISO plus LPS, or PGE plus LPS, leads to synergistic induction of many genes including GCSF, IL6 and IL10, and synergistic repression of genes including TNF α (Fig. 6b). These data support the model that ISO–PGE signalling modulates TLR signalling through a cAMP-dependent process that is comprised of an interaction

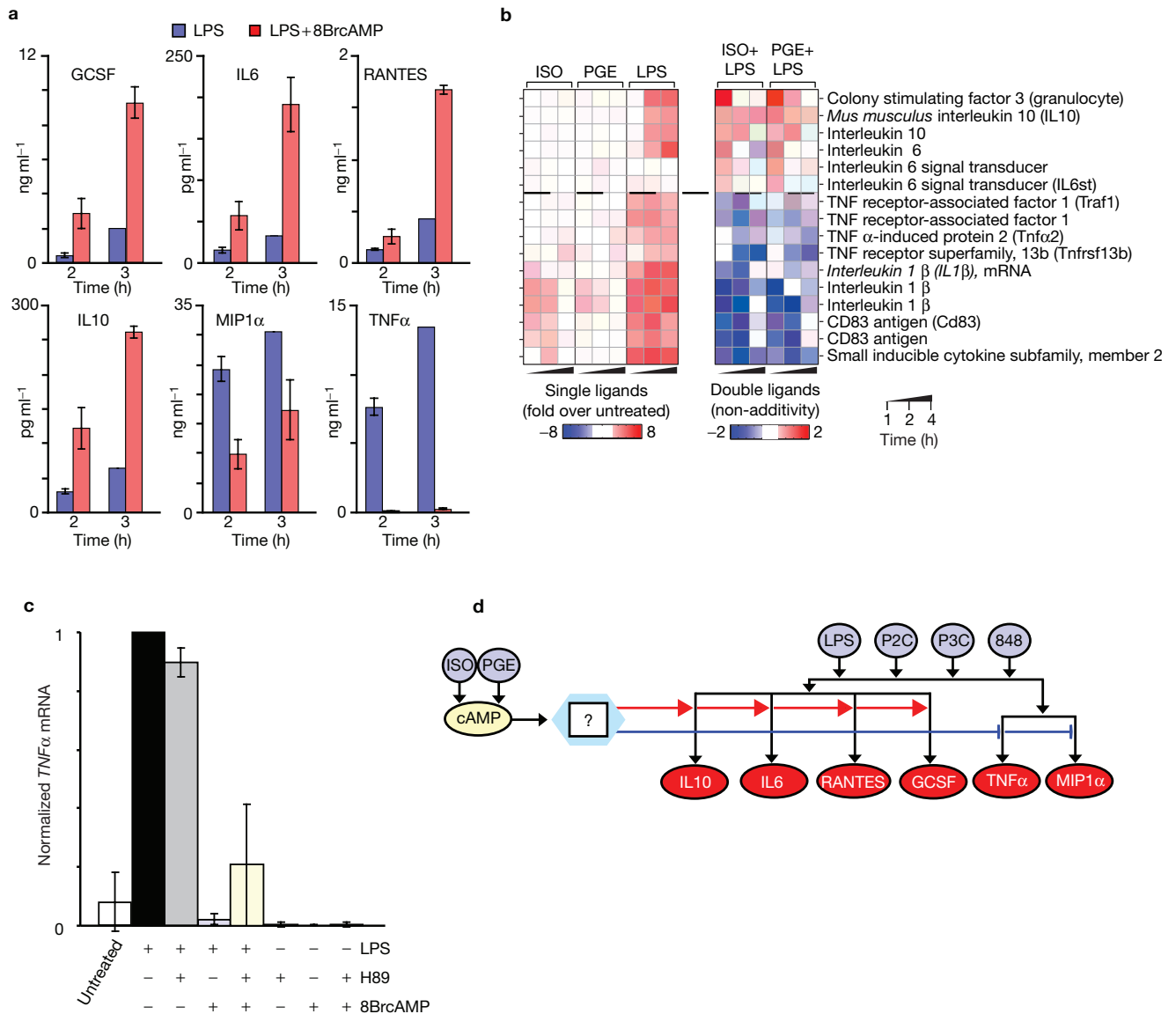


Figure 6 Testing the predicted interaction agent between G α s-GPCRs and TLRs. **(a)** GCSF, IL6, RANTES, IL10, MIP1 α and TNF α secretion at 2 and 3 h after stimulation by LPS (blue) or LPS+8BrcAMP (red; mean \pm s.d., $n = 2$, normalized to maximum LPS response). **(b)** The regulation of 21 genes (mean fold change over responses in untreated cells) in response to stimulation by each of ISO, PGE and LPS (30 microarrays; 1, 2 and 4 h) is shown in the left panel (red pixels indicate upregulation; white pixels indicate unchanged; blue pixels indicate downregulation). Some genes have the same descriptive names but have different nucleotide sequences (systematic names) on the chip. The panel on the right shows the non-additivity of responses to the pairs of ligands ISO + LPS and PGE + LPS (red pixels indicate synergy; blue pixels indicate inhibition). Note the systematic inhibitory influence of G α s on several members of the inflammatory cascade (for example, interleukin-1 β , cd83 antigen and mip2) that are upregulated

agent — a signalling circuit that provides generic communication between these signalling pathways and that is only exposed in the coincident activity of the pathways (Fig. 6d). From a biological point of view, this interaction agent makes sense; G α s-signalling in macrophage cells is known to attenuate the inflammatory response due to TLR activity^{16,21}.

To characterize possible cAMP-dependent processes that may be involved in this cross-talk, the effect of the PKA inhibitor H89 on the ability of 8BrcAMP to suppress LPS-dependent TNF α production was examined

by TLR signalling. **(c)** Levels of TNF α transcript assayed by quantitative RT-PCR 2 h after stimulation ($n = 3$, mean \pm s.d., normalized to maximum LPS response). The response to LPS (black) is completely inhibited in the presence of 8BrcAMP (light blue). This inhibition is not mediated by PKA as H89 does not significantly reduce the inhibition of 8BrcAMP on the LPS-induced TNF α response (light yellow). Controls responses to H89 (red), 8BrcAMP (light green) and H89 + 8BrcAMP (dark yellow) are not different from untreated cells (white) at 2 h. **(d)** A schematic representation of the interaction agent mediating cross-talk between G α s-GPCRs and TLRs. Colour convention is similar to Fig. 4d. TLR agonists induce secretion of multiple cytokines (red ovals). Stimulation of G α s-GPCRs selectively mediates both synergy and inhibition of TLR-induced cytokine responses through an unknown interaction agent (blue hexagon), that is independent of PKA activation in the regulation of at least one cytokine.

(Fig. 6c). The data show that H89 does not significantly affect the modulatory effect of cAMP on LPS signalling. Thus, at least with regard to the LPS-induced TNF α production, PKA is unlikely to be part of the cAMP-dependent modulatory cascade. These data show how the same signalling molecule (for example, cAMP) can be involved in multiple interaction agents. In this case, cAMP-dependent control of receptor-mediated Ca²⁺ mobilization occurs through a PKA-dependent process, and modulation of aspects of TLR signalling occurs through a PKA-independent process.

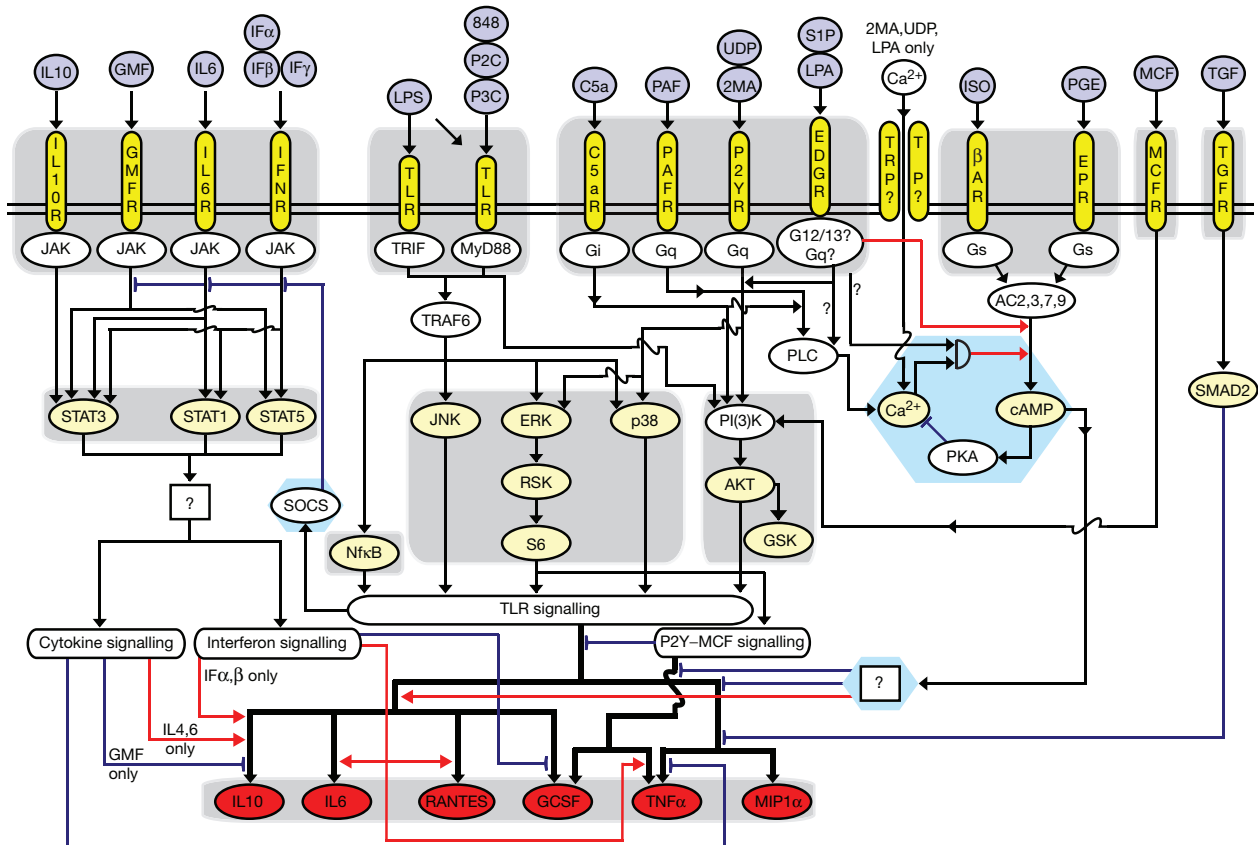


Figure 7 A schematic compilation of input–output relationships observed in the single and double-ligand screens. The representations follow previous examples (Figs 4d and 6d). Assayed parameters in the ligand screens are shown as light yellow ovals. Other known mechanisms (not assayed) are depicted as white ovals. Transcription factors (collectively described for each group of ligands, white rounded rectangles) are activated and undergo translocation

(thick black lines) to produce cytokines (red ovals), the final step in the input–output relationship. Interactions from the double ligand screen are shown as coloured arrows (red arrows indicate synergistic; blue arrows indicated less than additive). For visual clarity, interactions within groups are not displayed (for example, interactions between TLRs). Three interaction agents revealed by the double ligand screen are also indicated (blue hexagons).

Other clusters in the $\Delta\Delta Z$ matrix also support the notion of interaction agents. For example, clusters 2 and 3 reveal systematic pairwise interactions between interferon and TLR signalling pathways with regard to production of cytokines, a finding that is consistent with many other studies^{8–10}. Several mechanisms have been proposed for mediating such an interaction: first, up-regulation of TLRs by IFN signalling^{22–24}; second, potentiation of NF- κ B²⁵ and/or ERK and STAT²⁶ signalling pathways; and third, induction of the SOCS proteins^{27,28}, a family of regulatory molecules that are induced by TLR signalling and act to modulate JAK–STAT signalling such as through IFNs^{14,15}. Interestingly, the clustering pattern demonstrates similarities and difference between IFN β and IFN γ signalling in RAW 264.7 cells; both IFN β and IFN γ potentiate the production of IL-6 and RANTES by TLR signalling, but differ in that IFN β alone synergistically enhances IL-10 production, consistent with the known anti-inflammatory role specific for Type I interferons²⁹.

Based on these results, we propose that clustering of ligand interactions based on cytokine production originates from the existence of a limited set of interaction agents that provide the capacity to integrate specific signalling pathways to yield unique output responses. The relatively small number of clusters suggests the possibility that most of the combinatorial complexity of signalling may be accounted for by the convergence of signalling cascades on a small number of molecular mechanisms.

DISCUSSION

The work presented here provides initial insights into the architecture of the intracellular signalling machinery in the RAW 264.7 cells and provides important direction for further experimentation. A simplified picture (Fig. 7) of the signalling network that emerges from the single and double ligand screens serves to illustrate the basic results. Ligands taken individually cluster into specific response classes that reflect commonality in their early transduction mechanisms but fails to explain their physiological contribution to information processing. Taken in pairwise combinations, ligands begin to reveal their context-dependent roles in modulating final cellular outputs; indeed, the data suggest that the primary activity of many input ligands is modulation of other signalling systems rather than direct control over cellular outputs. The density of cross-talk demonstrates substantial capacity for encoding combinatorial complexity in input stimuli, but the clustering of non-additive response patterns places significant constraints on the mechanistic complexity of ligand interactions. We suggest that the topology of the signalling network in the RAW 264.7 cell is composed of modular transduction units representing the core transduction machinery downstream of specific receptor classes linked by a limited set of interaction agents whose number and promiscuity ultimately determine the processing complexity of the cell. The availability of an open access, high quality dataset of ligand responses, and the interactions between them in one cell type, should enable the signalling community to systematically test this hypothesis.

METHODS

Single-ligand responses. An error model was constructed for each data variable by collecting several datasets for mock-stimulated cells, which were defined as the reference (or basal) state. This provided a mean value and an expected variance for each variable with no applied stimulus. Each data variable collected on ligand stimulation was then expressed as the number of standard deviations removed from the error model (for example, the Z -score). Thus, for ligand i generating a value of a_i for the experimental variable x , the transformed representation of the value is given by:

$$Z_i^x = \frac{a_i - \bar{a}_{\text{basal}}}{\sigma_{\text{basal}}}$$

where Z_i^x is the significance of observing a_i given the error model. Multiple repeats of applying ligand i produced a distribution of Z -scores for variable x ; thus, the raw data variable is transformed into a mean Z -score with errors, and these are used to derive parameters for ligand similarity and interaction.

Double-ligand screen. This screen was used to identify cross-talk between ligands. Quantitatively, we define the ‘interaction’ of two ligands (1 and 2) on experiment variable x as:

$$\Delta\Delta Z_{1,2}^x = \frac{Z_{1,2}^x - (Z_1^x + Z_2^x)}{\sqrt{\sigma_{1,2}^2 + \sigma_1^2 + \sigma_2^2}}$$

where the difference between the observed effect of applying both ligands ($Z_{1,2}^x$) and the expected effect if they act independently ($Z_1^x + Z_2^x$) is weighted for the propagated errors of measurement. We note that $\Delta\Delta Z_{1,2}^x$ is not merely the difference between two ligand responses; it is a new parameter that gives the degree to which two ligands cooperatively determine each experiment variable. This interaction could arise from many sources and by itself says little about the underlying molecular mechanism. Nevertheless, it indicates complexity as it detects the context-dependence of specific output variables in the transduction of stimuli.

Clustering methods. All clustering was performed using implementations of hierarchical clustering in MATLAB (The Mathworks, Natick, MA). Distance calculations were made using the cityblock metric and linkages were established using the complete linkage method. Inconsistency coefficients³⁰ were calculated for each node in a dendrogram to rank the significance of clustering for the $\Delta\Delta Z$ matrix (Fig. 5). Briefly, an inconsistency coefficient of zero places every leaf node in a dendrogram in its own separate cluster while at the maximum inconsistency score all leaf nodes comprise a single cluster. To determine a threshold inconsistency score for partitioning leaf nodes in the $\Delta\Delta Z$ matrix into an optimal number of clusters the inconsistency scores for clustering the matrix were calculated following 1,000 trials of random permutation of the columns of the matrix. This randomization scrambled any similarities in patterns of non-additivity between ligand pairs; thus clustering in the randomized matrices is insignificant. A comparison of the number of clusters generated as a function of the inconsistency coefficient for the $\Delta\Delta Z$ matrix and the randomized trials provides the threshold value for cluster significance (see Supplementary Information, Fig. S3).

Experimental methods. Detailed protocols for the ligand screens developed by the AfCS are available online (<http://www.signaling-gateway.org/data/ProtocolLinks.html>). Brief summaries of key procedures are described in the Supplementary Methods.

cAMP assays. Intracellular cAMP levels were assayed identical to procedures in the ligand screen (AfCS Procedure Protocol ID: PP00000175) using an enzyme-linked immunoassay system (cAMP Biotrack EIA; Amersham Biosciences, Piscataway, NJ). Cells were stimulated with ISO (50 nM, Sigma-Aldrich, St Louis, MO), UDP (25 μ M, Sigma-Aldrich) or both. Stimulations with combinations of ISO + UDP were performed in the presence (pretreatment for 5 min) and absence of thapsigargin (1 μ M, Calbiochem, La Jolla, CA) or EGTA (2 mM, Sigma-Aldrich). Reactions were stopped at the times indicated after addition of stimulus and cAMP content was determined. To reduce day-to-day variability, cAMP levels on each day were normalized by area normalization of the ISO + UDP response for that experiment.

Calcium assays. Assay of intracellular calcium followed the same procedure as the ligand screen experiments (AfCS Procedure Protocol ID: PP00000176). Cells were stimulated with C5a (100 nM, Calbiochem) in the absence and presence of 8BrcAMP (2 mM, Sigma-Aldrich), H89 (12.5 μ M, Biomol, Plymouth Meeting, PA) or both. Cells were pretreated with 8BrcAMP and H89 5 min and 10 min before C5a stimulation, respectively. Data were normalized to the peak of the C5a response for comparison.

Cytokine assays. Assay of cytokine secretion followed the same procedure as the ligand screen experiments (AfCS Procedure Protocol ID PP00000209, -221, -223). Cells were stimulated with LPS (100 ng ml⁻¹, Sigma-Aldrich; all LPS treatments were made with added LBP 250 pM, R&D Systems, Minneapolis, MN) or with a combination of LPS and 8BrcAMP (1 mM). Supernatants were collected at 2 and 3 h after initiation of stimulation and assayed for cytokine content. Data were normalized to the maximum secretion of each cytokine in response to LPS treatment alone. For estimation of cytokine mRNA levels, cells treated as above were lysed for mRNA extraction (RNeasy plus mini kit, Qiagen, Valencia, CA) and subsequent cDNA synthesis (Copy kit, Invitrogen, Carlsbad, CA) that was used as template for quantitative RT-PCR reactions. Primers for the TNF α gene were designed using Primer3 (ref. 31) based on design constraints of melting temperatures >60 °C, GC content >50% and size <30 base pairs (bp), with the final product spanning at least two introns (275 bp). The following primers were used: 2R-TNF α , TACGACGTGGGCTACAGGCTTG; 2F-TNF α , GAAAGCATGATCCGCGACGTGGA. A reference gene (18S) and reference cDNA synthesized from RNA isolated from total spleen (a kind gift from J. Lee, UTSMC) were used for normalization for each reaction. Day-to-day variability between experiments was reduced by normalizing to maximum LPS response.

Microarray experiments. Publicly available AfCS microarray data was used to examine interactions between ligands. Data from 30 AfCS microarray experiments (five ligands; ISO, PGE, LPS, ISO + LPS and PGE + LPS at three time-points (1, 2 and 4 h), repeated twice; see Supplementary Information, Table S1 for ligand details) were downloaded and analyzed using custom scripts written in MATLAB (R14, The Mathworks).

Note: Supplementary Information is available on the Nature Cell Biology website.

ACKNOWLEDGEMENTS

We are indebted to the many individuals from several academic institutes that are members of the AfCS scientific team for data collection, for database construction and for providing general help and advice. This work would not have been possible without the transparent and efficient public access to raw experimental data supported by the AfCS effort. We also thank members of the AfCS steering committee and the Ranganathan lab for discussion and critical reading of the manuscript. Work on this project was supported by contributions from public and private sources, including the NIGMS Glue Grant Initiative (U54 GM062114). A complete listing of the AfCS sponsors can be found at <http://www.signaling-gateway.org/aboutus/sponsors.html>. R.R. acknowledges support from the Mallinckrodt Scholar award, the Keck Future Initiatives award and the Robert A. Welch Foundation, and is an investigator of the Howard Hughes Medical Institute. P.C.S. acknowledges support from the Robert A. Welch Foundation and is the Alfred and Mabel Gilman Chair in molecular pharmacology.

COMPETING FINANCIAL INTERESTS

The authors declare that they have no competing financial interests.

Published online at <http://www.nature.com/naturecellbiology/>
Reprints and permissions information is available online at <http://npg.nature.com/reprintsandpermissions/>

1. Gilman, A. G. *et al.* Overview of the Alliance for Cellular Signaling. *Nature* **420**, 703–706 (2002).
2. Akira, S., Yamamoto, M. & Takeda, K. Role of adapters in Toll-like receptor signalling. *Biochem. Soc. Trans.* **31**, 637–642 (2003).
3. Ihle, J. N. Cytokine receptor signalling. *Nature* **377**, 591–594 (1995).
4. Chen, Z. P., Levy, A. & Lightman, S. L. Nucleotides as extracellular signalling molecules. *J. Neuroendocrinol.* **7**, 83–96 (1995).
5. Chen, L. W., Lin, M. W. & Hsu, C. M. Different pathways leading to activation of extracellular signal-regulated kinase and p38 MAP kinase by formyl-methionyl-leucyl-phenylalanine or platelet activating factor in human neutrophils. *J. Biomed. Sci.* **12**, 311–319 (2005).
6. Sato, S. *et al.* Synergy and cross-tolerance between toll-like receptor (TLR) 2- and TLR4-mediated signaling pathways. *J. Immunol.* **165**, 7096–7101 (2000).

7. Medvedev, A. E., Kopydlowski, K. M. & Vogel, S. N. Inhibition of lipopolysaccharide-induced signal transduction in endotoxin-tolerized mouse macrophages: dysregulation of cytokine, chemokine, and toll-like receptor 2 and 4 gene expression. *J. Immunol.* **164**, 5564–5574 (2000).
8. Hemmi, H. *et al.* The roles of two I κ B kinase-related kinases in lipopolysaccharide and double stranded RNA signaling and viral infection. *J. Exp. Med.* **199**, 1641–1650 (2004).
9. Hausler, K. G. *et al.* Interferon γ differentially modulates the release of cytokines and chemokines in lipopolysaccharide- and pneumococcal cell wall-stimulated mouse microglia and macrophages. *Eur. J. Neurosci.* **16**, 2113–2122 (2002).
10. Yamamoto, M. *et al.* Cutting edge: a novel Toll/IL-1 receptor domain-containing adapter that preferentially activates the IFN- β promoter in the Toll-like receptor signaling. *J. Immunol.* **169**, 6668–6672 (2002).
11. Gessani, S., Belardelli, F., Pecorelli, A., Puddu, P. & Baglioni, C. Bacterial lipopolysaccharide and γ -interferon induce transcription of β -interferon mRNA and interferon secretion in murine macrophages. *J. Virol.* **63**, 2785–2789 (1989).
12. Tilg, H. & Kaser, A. Type I interferons and their therapeutic role in Th2-regulated inflammatory disorders. *Expert Opin. Biol. Ther.* **4**, 469–481 (2004).
13. Aderka, D., Le, J. & Vilcek, J. IL-6 inhibits lipopolysaccharide-induced tumor necrosis factor production in cultured human monocytes, U937 cells, and in mice. *J. Immunol.* **143**, 3517–3523 (1989).
14. Heeg, K. & Dalpke, A. TLR-induced negative regulatory circuits: role of suppressor of cytokine signaling (SOCS) proteins in innate immunity. *Vaccine* **21**, S61–S67 (2003).
15. Niemand, C. *et al.* Activation of STAT3 by IL-6 and IL-10 in primary human macrophages is differentially modulated by suppressor of cytokine signaling 3. *J. Immunol.* **170**, 3263–3272 (2003).
16. Zhang, H. *et al.* Effect of adrenoreceptors on endotoxin-induced cytokines and lipid peroxidation in lung explants. *Am. J. Respir. Crit. Care Med.* **160**, 1703–1710 (1999).
17. Lukashov, D., Ohta, A., Apasov, S., Chen, J. F. & Sitkovsky, M. Cutting edge: Physiologic attenuation of proinflammatory transcription by the Gs protein-coupled A2A adenosine receptor *in vivo*. *J. Immunol.* **173**, 21–24 (2004).
18. O'Donnell, P. M. & Taffet, S. M. The proximal promoter region is essential for lipopolysaccharide induction and cyclic AMP inhibition of mouse tumor necrosis factor- α . *J. Interferon Cytokine Res.* **22**, 539–548 (2002).
19. Hareng, L., Meergans, T., von Aulock, S., Volk, H. D. & Hartung, T. Cyclic AMP increases endogenous granulocyte colony-stimulating factor formation in monocytes and THP-1 macrophages despite attenuated TNF- α formation. *Eur. J. Immunol.* **33**, 2287–2296 (2003).
20. Akaogi, J. *et al.* Prostaglandin E2 receptors EP2 and EP4 are up-regulated in peritoneal macrophages and joints of pristane-treated mice and modulate TNF- α and IL-6 production. *J. Leukoc. Biol.* **76**, 227–236 (2004).
21. Farmer, P. & Pugin, J. β -adrenergic agonists exert their 'anti-inflammatory' effects in monocytic cells through the I κ B/NF- κ B pathway. *Am. J. Physiol. Lung Cell Mol. Physiol.* **279**, L675–L682 (2000).
22. Nansen, A. & Randrup Thomsen, A. Viral infection causes rapid sensitization to lipopolysaccharide: central role of IFN- α β . *J. Immunol.* **166**, 982–988 (2001).
23. Durbin, J. *et al.* The role of STAT1 in viral sensitization to LPS. *J. Endotoxin. Res.* **9**, 313–316 (2003).
24. Hertzog, P. J., O'Neill, L. A. & Hamilton, J. A. The interferon in TLR signaling: more than just antiviral. *Trends Immunol.* **24**, 534–539 (2003).
25. Harada, K., Isse, K. & Nakanuma, Y. Interferon gamma accelerates NF- κ B activation of biliary epithelial cells induced by Toll-like receptor and ligand interaction. *J. Clin. Pathol.* **59**, 184–190 (2006).
26. Zhao, J. *et al.* IRF-8/ICSBP is involved in TLR signaling and contributes to the cross talk between TLR and IFN- γ signaling pathways. *J. Biol. Chem.* **281**, 10073–10080 (2006).
27. Baetz, A., Frey, M., Heeg, K. & Dalpke, A. H. Suppressor of cytokine signaling (SOCS) proteins indirectly regulate toll-like receptor signaling in innate immune cells. *J. Biol. Chem.* **279**, 54708–54715 (2004).
28. Dalpke, A. H. & Heeg, K. Synergistic and antagonistic interactions between LPS and superantigens. *J. Endotoxin Res.* **9**, 51–54 (2003).
29. Vandeusen, J. B. *et al.* STAT-1-mediated repression of monocyte interleukin-10 gene expression *in vivo*. *Eur. J. Immunol.* **36**, 623–630 (2006).
30. Mojena, R. Hierarchical grouping methods and stopping rules: An evaluation. *Computer J.* **20**, 359–363 (1977).
31. Rozen, S. & Skaletsky, H. Primer3 on the WWW for general users and for biologist programmers. *Methods Mol. Biol.* **132**, 365–386 (2000).